Operational Optimization of an Agricultural Microgrid

Paul D. Brown
Department of Electrical and Electronics Engineering
Middle East Technical University
Ankara, Turkey
ORCID: 0000-0001-5753-0449

Murat Göl
Department of Electrical and Electronics Engineering
Middle East Technical University
Ankara, Turkey
ORCID: 0000-0002-2523-1169

***Abstract*—A demonstration agricultural microgrid containing solar photovoltaic (PV), battery storage system (BSS) and multiple water pumps and reservoirs is presented. A mathematical model of the cost of operating the demonstration microgrid is developed. The mathematical model includes hybrid inverter source switching and BSS charging modes in addition to power balance and inter-period energy and water-level coupling. Electricity pricing and irrigation water use efficiency are allowed to vary by time of day. The mathematical model is formulated as a mixed-integer linear program (MILP), implemented in Python using Pyomo, and optimized using the open-source SCIP solver to plan pumping and water usage. Estimated data for a demonstration system at a farm in Turkey is used to demonstrate the proposed model. Results of the optimization of the demonstration system show intuitive results that are superior to a rule-based initialization. The model may serve as the basis for model predictive control (MPC) or stochastic model predictive control (SMPC).**

***Index Terms*—Microgrid, optimization, photovoltaic systems, energy storage, irrigation**

I. Introduction

Many factors are driving change within the electrical power industry over recent decades. One such trend is the ongoing electrification of rural regions around the globe. For agricultural consumers, electrification enables increased yields and economic development. Ref. [1] reviews technology and applications for off-grid systems for rural electrification.

Use of solar photovoltaic (PV) and other renewable distributed energy resources (DER) facilitates rural electrification by reducing the infrastructure cost required. PV energy is generally well aligned with water needs [2]. Ref. [2] reviews numerous solar-powered water pumping applications around the world while [3] reviews the PV and water pumping modeling, design, and control approaches in the literature.

In recent years, much research has been done into the benefits and issues related to microgrids [4], [5]. While microgrids can facilitate rural electrification by allowing connection of loads and distributed energy sources with or without a connection to the main grid, development of microgrids requires new techniques for planning, control, and operation [6], [7].

Much of the literature regarding optimization of microgrids has focused on design optimization and optimal sizing of system components [6], [8]. Ref. [9] investigates the optimal operation of a microgrid including pumped hydro energy storage by formulating a non-linear optimization problem and using the two-point estimate method (TPEM) to account for uncertainty. In [10], the authors evaluate three rule-based control strategies using the HOMER Pro microgrid analysis tool. Ref. [11] proposes a MPC for battery energy storage system (BESS) associated with a grid-connected PV system. The proposed control scheme determines the BESS power schedule, maximizing profit from real-time energy price arbitrage by time-shifting while accounting for BESS costs associated with cycling and smoothing the plant and BESS output.

This paper focuses on the operational planning of an agricultural microgrid with a grid connection, a DER (PV), irrigation pumping load, and water and electrical energy storage. This paper presents an original mathematical formulation of the operational optimization problem suitable for model-predictive control (MPC) of an agricultural microgrid. The novelty of this work is the inclusion of PV and water needs as well as the modeling of the hybrid inverter source switching and BSS charging modes.

In this paper, Section II briefly describes the demonstration system that is modeled. Then in Section III, the mathematical formulation of the problem is presented. Data used for the demonstration system is shown in Section IV. Implementation details are provided in Section V. In Section VI, results of the optimization for the demonstration system data is shown. Section VII describes some conclusions and directions for future work.

II. Demonstration System

The optimization problem is specifically formulated for a demonstration system to be installed at the Güneşköy farm [12]. A block diagram of the demonstration system with anticipated component ratings is shown in Fig. 1.

The existing pump will continue to be fed from the grid. The site electrical load will be fed from a hybrid inverter [13] that will have battery, PV, and grid connections available. A new pump load will be fed from an inverter drive [14] connected to the PV DC bus.

The power flow directions within the demonstration system are shown in Fig. 2.

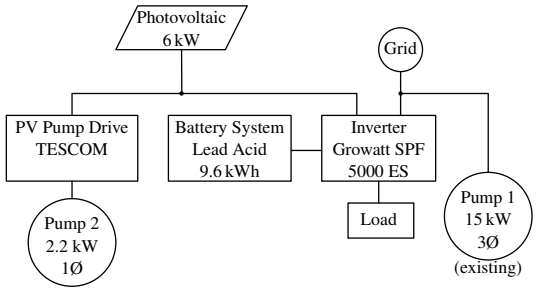

Fig. 1. Güneşköy Demonstration System

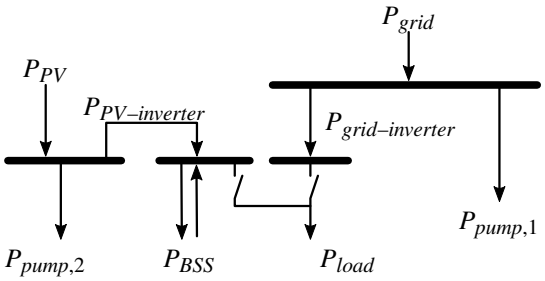

Fig. 2. Microgrid power flows

III. Problem formulation

The problem variables, objective function, and constraints are described in the following subsections. Refer to Tables I to III for definitions of the symbols used.

A. Problem variables

The problem variables are shown in Table I. The optimization determines the best times to run Pump 1, when and how much to run Pump 2, and when to utilize water for irrigation.

B. Objective function

The objective function includes several components and is shown in (1). The actual cost component is the cost of grid power. The cost of battery usage component represents the portion of the replacement cost of the battery system incurred due to the loss of life caused by battery cycling [15]. The other penalty factors encourage the full supply of desired water on each day and discourage unnecessary switching of the BSS mode and Pump 1 respectively.

TABLE I
Problem variables

Symbol	Description	Units
$s_{pump1,t}$	Pump 1 on-off selection variable[3]	-
$P_{pump2,t}$	Power used for pumping water to Reservoir 2	W
$Q_{use,r,t}$	Flow of water used (irrigation or other use) from Reservoir r	m^3/h

[1] Variables subscripted with t have a value for each time period.
[2] Variables subscripted with r have a value for each reservoir.
[3] Binary variable. 1: Running. 0: Off.

TABLE II
Calculated quantities

Symbol	Description	Units
$P_{pump1,t}$	Power used by Pump 1 for pumping water to Reservoir 1	W
$Q_{pump,r,t}$	Volume of water pumped by Pump r	m^3
$s_{BSS,t}$	Operating mode of BSS[4]	-
$P_{BSS,ch,t}$	Power used to charge the BSS	W
$P_{BSS,disch,t}$	Power drawn from discharging the BSS	W
$s_{inv,t}$	Inverter mode[5]	-
$P_{PV,t}$	Power drawn from the PV array	W
$P_{PV-inverter,t}$	Power flow from the PV bus to the inverter	W
$P_{grid,t}$	Power from the electrical grid	W
$P_{grid-inverter,t}$	Power from the grid to the hybrid inverter	W
$E_{BSS,t}$	Energy stored in the BSS at the end of the period	Wh
$V_{w,r,t}$	Volume of water stored at the end of the period	m^3
$V_{use,d}$	Effectively used volume of water (irrigation or other use) on day d	m^3

[1] Variables subscripted with t have a value for each time period
[2] Variables subscripted with r have a value for each reservoir
[3] Binary variable. 1: Charging. 0: Discharging.
[4] Binary variable. 1: Inverter fed from utility source. 0: Inverter fed from BSS/PV source.

$$
\begin{aligned}
&\min \underbrace{\sum_t C_{grid,t}\ P_{grid,t}\ \Delta t}_{\text{Cost of grid power}} \\
&+ \underbrace{\sum_t C_{BSS}\left(P_{BSS,ch,t} + P_{BSS,disch,t}\right)\Delta t}_{\text{Cost of battery usage}} \\
&+ \underbrace{C_{w,short}\sum_d \max\left(\left(V_{use,desired,d} - V_{use,d}\right), 0\right)}_{\text{Penalty for inadequate water}} \\
&+ \underbrace{C_{BSS,switching}\sum_t \left|s_{BSS,t} - s_{BSS,t-1}\right|}_{\text{BSS mode-switching penalty}} \\
&+ \underbrace{C_{Pump1,switching}\sum_t \left|s_{pump1,t} - s_{pump1,t-1}\right|}_{\text{Pump 1 switching penalty}}
\end{aligned}
\tag{1}
$$

C. Constraints

The constraints represent mathematically the operation and allowable states of the microgrid system. The constraints related to each component of the microgrid are as follows:

TABLE III
PROBLEM PARAMETERS / DATA

Symbol	Description	Units
$P_{load,t}$	Power drawn by electrical loads	W
$P_{PV,avail,t}$	Power available from PV array (MPP)	W
$P_{pump1,max}$	Operating power of Pump 1	W
$s_{pump1,0}$	Initial state of Pump 1	-
Q_{w1}	Fixed water flow for Pump 1	m^3/h
$P_{pump2,min}$	Minimum operating power of Pump 2	W
$P_{pump2,max}$	Maximum operating power of Pump 2	W
$Q_{w2}\left(P_{pump2}\right)$	Function relating pumped water quantity to electrical power for Pump 2	m^3/h
$P_{BSS,ch,max}$	Bulk charging power for the BSS	W
$P_{BSS,disch,max}$	Maximum power for discharging the BSS	W
K_{BSS}	BSS absorption mode charge rate constant	-
$E_{BSS,0}$	Initial value of energy stored in the BSS	Wh
$s_{inv,0}$	Initial state of inverter	-
$E_{BSS,max}$	Maximum energy that can be stored in the BSS	Wh
$E_{BSS,lower}$	Inverter threshold to switch from BSS/PV source to utility source	W
$E_{BSS,upper}$	Inverter threshold to switch from utility source to BSS/PV source	W
$V_{w,r,0}$	Initial value of water stored	m^3
$V_{w,r,min}$	Minimum volume of water	m^3
$V_{w,r,max}$	Maximum volume of water	m^3
$V_{use,desired,d}$	Desired volume of effectively used water on day d	m^3
D_d	Set of time periods t belonging to day d.	-
$Q_{use,r,max}$	Maximum rate of water use	m^3/h
$C_{grid,t}$	Cost of power from the grid	\$/Wh
C_{BSS}	Cost of storing power in the BSS	\$/Wh
$C_{BSS,switching}$	Penalty for changing BSS charging/discharging mode	\$/ea
$C_{w,short}$	Cost or penalty factor for water that is desired but not used	$\$/m^3$
η_{BSS}	Efficiency of BSS in charging or discharging	-
$\eta_{w,t}$	Efficiency of water use	-
Δt	Time interval for discretized planning horizon	h

[1] Parameters subscripted with t have a value for each time period
[2] Parameters subscripted with r have a value for each reservoir

1) Power Balance: There is a power balance constraint equation for each of the four buses shown in Fig. 2. Equation (2) enforces balance on the PV bus, (3) enforces balance in the hybrid inverter PV/BSS side, (4) enforces balance in the hybrid inverter grid side, and (5) enforces balance on the grid-side bus.

$$P_{PV,t} - P_{pump2,t} - P_{PV-inverter,t} = 0 \tag{2}$$

$$P_{PV-inverter,t} + P_{BSS,disch,t} - P_{BSS,ch,t} - \left(1 - s_{inv,t}\right)\ P_{load,t} = 0 \tag{3}$$

$$P_{grid-inverter,t} = s_{inv,t}\ P_{load,t} \tag{4}$$

$$P_{grid,t} - P_{grid-inverter,t} - P_{pump1,t} = 0 \tag{5}$$

The direction of power flow from the PV bus to the inverter and from the grid to the inverter are constrained to be positive as shown in (6) and (7).

$$0 \leq P_{PV-inverter,t} \tag{6}$$

$$0 \leq P_{grid-inverter,t} \tag{7}$$

2) Photovoltaic: It is assumed that the microgrid has the ability to track the photovoltaic array maximum power point (MPP) regardless of the operation of either or both of the hybrid inverter and the drive for Pump 2. It is also assumed that the control system has the ability to know what the maximum available PV power is, even if the system is not operating at the MPP. The full available output of the PV system may not be used if the load is less than the available PV power.

$$0 \leq P_{PV,t} \leq P_{PV,avail,t} \tag{8}$$

3) Pumps: Pump 1 is operated in a simple on-off fashion at a fixed power level.

$$P_{pump1,t} = s_{pump1,t}\ P_{pump1,max} \tag{9}$$

$$Q_{pump1,t} = s_{pump1,t}\ Q_{w1} \tag{10}$$

It is assumed that Pump 2 may be operated at a specified range-limited power setpoint chosen by the controller. The pumping power $P_{pump2,t}$ is a semi-continuous variable, being continuous between a minimum and a maximum or else 0.

$$P_{pump2,t} = 0 \ \vee\ P_{pump2,min} \leq P_{pump2,t} \leq P_{pump2,max} \tag{11}$$

$$Q_{pump2,t} = Q_{w2}\left(P_{pump2,t}\right) \tag{12}$$

Equation (13) is a placeholder for the currently unknown relationship between pump flow and power. For real-time control, the EMS controller could infer this relationship by observing the operation of the pump. Until then, a simple linear efficiency coefficient η_{pump2} is used to characterize the power-flow relationship of Pump 2 as shown in (13), where h is the head in m, ρ is the density of the water being pumped in kg/m^3, and g is the acceleration of gravity in m/s^2.

$$Q_{w2}\left(P_{pump2,t}\right) = \frac{P_{pump2,t}\ \eta_{pump2}}{h\rho g} \tag{13}$$

4) Hybrid Inverter and BSS: The hybrid inverter selected for the demonstration system at Güneşköy has limited capability to receive external control. It is assumed that the hybrid inverter will be configured with a priority order for supplying load such that the load will be supplied from PV if available, supplemented by power from the BSS. If PV is not sufficient and the BSS charge level is too low, then the utility grid source will be used. It is assumed that the hybrid inverter will charge the BSS only from PV and not from the utility grid source.

It is planned for the BSS to consist of lead-acid batteries. The hybrid inverter is responsible for charging the lead-acid battery bank. The inverter uses a four-stage charging cycle [14]:

1) **Bulk charging.** Charges at a settable maximum charging current. The power to the battery is nearly constant and is approximated in this formulation as a constant power $P_{BSS,ch,max}$.
2) **Absorption charging.** Once the voltage reaches the set maximum charging voltage, the voltage is held for a duration of 10 times the time spent in bulk charging mode. The power to the battery declines exponentially with time as the BSS voltage approaches the charging voltage and the SOC approaches 100%.

3) **Float charging.** Once the absorption charge timer completes, the charger switches to float charging mode in which a fixed voltage is held and minimal charging current is output except to compensate the small battery internal discharge or load discharging of the battery.
4) **Equalization charging.** Equalization charging is only applicable to flooded lead acid batteries and not to sealed lead acid batteries. In this mode, the battery is temporarily overcharged in order to reduce sulfation on the battery plates.

For the purposes of a mathematical model of the hybrid inverter's battery charging system for this optimization problem, only the bulk charging and absorption charging modes are represented. The other charging modes are neglected since little energy transfer to the BSS is completed these modes.

Equation (14) forces the charger state to charging mode if power is available. Equation (15) enforces the limit for absorption charging mode of the hybrid inverter, limits charging power to available power from the PV after meeting pumping and load power, and only allows charging when $s_{BSS,t}$ is in charging mode. Equation (16) only allows discharging when $s_{BSS,t}$ is in discharging mode.

$$s_{BSS,t} = \left(P_{PV,avail,t} - P_{pump2,t} - (1 - s_{inv,t})P_{load,t} \geq 0\right) \quad (14)$$

$$P_{BSS,ch,t} = \min\Bigg(\underbrace{K_{BSS}\ \frac{E_{BSS,max} - E_{BSS,t-1}}{\eta_{BSS}\ \Delta t}}_{\text{Absorption mode charging limit}}, \underbrace{P_{PV,avail,t} - P_{pump2,t} - (1 - s_{inv,t})P_{load,t}}_{\text{Unused available PV power}}, \underbrace{s_{BSS,t}\ P_{BSS,ch,max}}_{\text{Enforce charger mode}} \Bigg) \quad (15)$$

$$0 \leq P_{BSS,disch,t} \leq \left(1 - s_{BSS,t}\right) P_{BSS,disch,max} \quad (16)$$

The constant K_{BSS} takes a value between 0 and 1 and determines this switchover point from bulk charging mode to absorption charging and the rate of decrease in the charging power in absorption charging mode. A K_{BSS} value of 1 indicates that the charger remains in bulk charging mode until the BSS is fully charged.

According to the the hybrid inverter user manual [14], when in "SBU priority" mode, the hybrid inverter switches from PV/battery source to utility source when the battery goes below a minimum voltage level and switches back to the battery when the battery rises above a minimum voltage level. Equation (17) represents this logic to determine the connection of the inverter in time period t based on the connection during the previous period and the BSS energy level at the end of the previous period. Modeled this way, the mode is switched only at discrete time intervals, so the model will show the battery BSS charge level will going a little above and below the set thresholds rather than switching mid-period as the actual hybrid inverter will do.

$$s_{inv,t} = \left(s_{inv,t-1} \text{ and } \left(E_{BSS,t-1} \leq E_{BSS,upper}\right)\right) \text{ or } \left(E_{BSS,t-1} \leq E_{BSS,lower}\right) \quad (17)$$

Equation (18) couples the battery system energy balance from one period to the next. It includes a factor for conversion losses on energy input and energy output.

$$E_{BSS,t} = E_{BSS,t-1} + P_{BSS,ch,t}\ \eta_{BSS}\ \Delta t - \frac{P_{BSS,disch,t}\ \Delta t}{\eta_{BSS}} \quad (18)$$

5) Water Flow: Equation (19) couple the water level in the reservoirs from one period to the next.

$$V_{w,r,t} = V_{w,r,t-1} + Q_{pump,r,t}\ \Delta t - Q_{use,r,t}\Delta t \quad (19)$$

Equation (20) sums the effective irrigation water across periods in each day, taking into consideration the varying efficiency of irrigation in different periods. It is assumed that water use between the reservoirs is interchangeable.

$$V_{use,d} = \sum_{t \in D_d} \sum_{r} \eta_{w,t} Q_{use,r,t} \Delta t \quad (20)$$

Equations (21) and (22) are the limits on feasible values of the water flow and reservoir level values.

$$0 \leq Q_{use,r,t} \leq Q_{use,r,max} \quad (21)$$

$$V_{w,r,min} \leq V_{w,r,t} \leq V_{w,r,max} \quad (22)$$

IV. Data Values

Data for the problem parameters was estimated based on the planned demonstration system shown in Fig. 1. While the parameters used are intended to represent a realistic system, they have not been validated operationally. Full details of all parameters used may be found in the source code archive for this paper, released on GitHub [16] and CodeOcean [17].

Grid energy costs $C_{grid,t}$ were set for the daytime, peak, and nighttime rates and daily periods that Güneşköy was billed at in 2020, not including fees for power factor, etc., converted to US Dollars at approximately the Turkish Lira-US Dollar exchange rate that was effective at the time. Cost parameters for C_{BSS}, $C_{w,short}$, $C_{BSS,switching}$, $C_{Pump1,switching}$ were arbitrarily set to 0.01, 100, 1, and 1 respectively.

Water usage efficiency $\eta_{w,t}$ was set using different values for each hour of the day, with the highest efficiency (1.0) during nighttime hours and the lowest efficiency (0.5) during early afternoon.

Random values were generated for the load and the desired water use. Load was drawn from a uniform distribution ranging from 0 to 1 kW. Daily desired water use was drawn from a normal distribution with a mean of 140 m^3 and a standard deviation of 60 m^3. The generator for the pseudo-random number series was initialized using a seed value to ensure reproducibility.

Pump, battery, and PV parameters were selected to represent the demonstration system shown in Fig. 1. The hybrid inverter source selection was configured to stay on the PV/BSS source until the BSS charge dropped below 30% and then switch to the grid to charge until it reached a charge level of 95%. The BSS charging and discharging efficiency was set to 95%. Hourly averages of the recorded output power of the rooftop PV array on the METU EEE Department machinery building

TABLE IV
OBJECTIVE FUNCTION COMPONENTS

	Initialized ($, 2020)	Optimized ($, 2020)
Grid energy cost	2448.1	1192.4
Battery use cost	198.6	326.1
Inadequate water cost	0.0	0.0
Battery mode switching cost	8.0	7.0
Pump switching cost	1.0	2.0
TOTAL	2655.7	1526.5

were scaled to the rating of the demonstration system and used for the available PV power.

The optimization period was set for a length of 72 h with a time step Δt of 1 h used. The time period of 72 h (3 days) was used so that the optimizer wouldn't use up all the stored water and energy to meet the needs of the first day, neglecting its benefit for future days. Initial values for E_{BSS}, V_{w1}, V_{w2}, and s_{inv} were set randomly. The results shown in Section VI are from the simulation starting on 24 February 2021.

V. IMPLEMENTATION

The problem was modeled in the Python programming language using the Pyomo library [18], [19] and solved using the SCIP [20] open-source mixed-integer linear program (MILP) solver. In order to use a MILP solver, auxiliary binary variables were introduced to linearize non-linear functions such as max, min, absolute value, $\geq$, $\leq$, and logic functions and and or. The formulation of the non-linear functions was based on [21] and original work by the author. Semi-continuous variables were modeled using the approach described in [22].

The problem, solved for a time period of 72 h with an interval Δt of 1 h, contained a total of 938 continuous and 1008 binary variables. SCIP converged to a solution in less than 40 seconds.

Initialization to a feasible point was performed using a single forward-pass heuristic of greedy pumping with Pump 2 if PV was available, then meeting loads with PV and BSS energy, discharging BSS to meet loads if necessarily and energy was available. Initial Pump 1 pumping and water use was set by iteratively solving a linear problem to try to add pumping one hour at a time until the desired water usage was met. The linear initialization problem was implemented in Pyomo and solved using GLPK [23].

VI. RESULTS

The optimization run reduced the cost of the objective function from the initialized value of of $2655.7 to an optimized value of $1526.5. The components of the initialized and optimized objective function costs are shown in Table IV. The proposed model improves upon a simple priority-based heuristic by allowing the optimizer to minimize the operating cost by pumping water or BSS charging or some of both.

Fig. 3 shows the power on the PV and BSS side of the microgrid. Due to the relative ratings of the PV array, Pump 2, and the BSS, on the sunny days (24 and 26 February), the full available PV power is not able to be used. The optimal operation does not strictly prefer pumping water or charging the BSS. Instead, the BSS is charged enough to prevent the hybrid inverter from switching back to the grid.

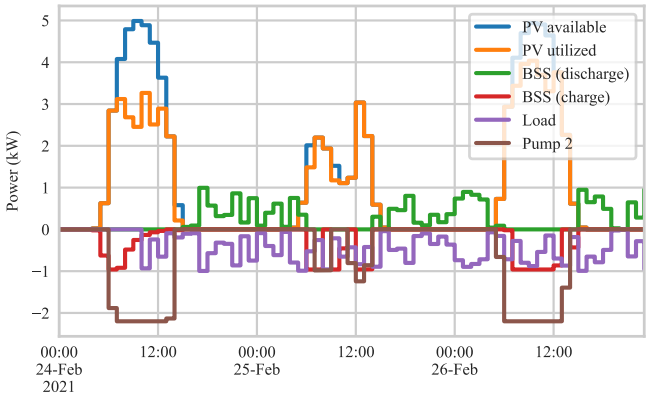

Fig. 3. PV-Side Power

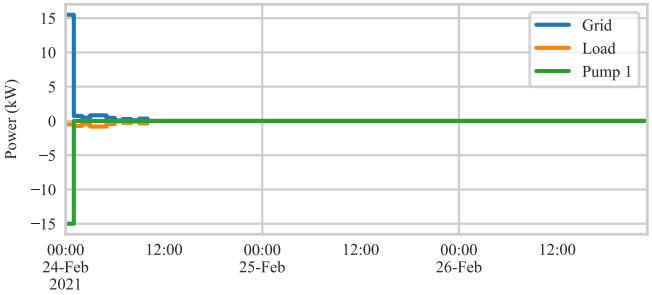

Fig. 4. Grid-Side Power

Fig. 4 shows the power on the grid side of the microgrid. On the first day (24 February), the hybrid inverter starts initially connected to the grid. As shown in Fig. 5, once the BSS is recharged by PV during the day, the hybrid inverter switches to the PV/BSS source and is able to supply the load for the rest of the modeled period. The largest load on the grid is Pump 1, which optimally runs during the nighttime hours where time-of-day electrical rates are cheapest.

Fig. 6 shows the water level in the two reservoirs. Since the efficiency of water usage is highest at night, the optimal operation releases water during the nighttime hours.

VII. CONCLUSION

This paper has presented a detailed mathematical model for an agricultural microgrid suitable for optimization of the operation of the pumps and water usage. The model was implemented in open-source software and results have been presented.

The model is not intended to stand alone but to serve as one component of a microgrid energy management system (EMS). One possible application of this model is for use in model-predictive control (MPC) of the microgrid. In such a scheme, the system operation is optimized over some time horizon,

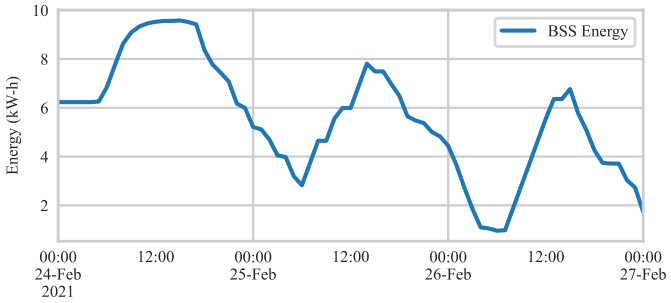

Fig. 5. BSS Energy Stored

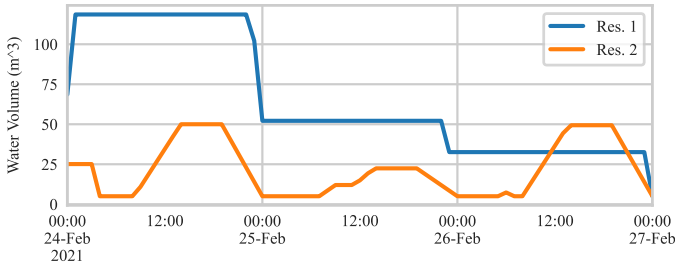

Fig. 6. Water Stored

but only the first step is used as the control output. The time horizon is then slid forward one step and the optimization is repeated.

In the formulation presented in this paper, a single value represents each of the parameters, including available PV power, loads, and desired water volume, all of which are dependent on random processes. One possible extension of this model would be to make it stochastic so that multiple possible future scenarios are represented. Unlike in standard MPC, where the output of the optimization problem is the control input (feed-forward), in stochastic model predictive control (SMPC), the output of the optimization problem is the optimal control law to be applied in the future time periods [24]. Thus, the system is able to respond to stochastic events dynamically without having to re-run the MPC problem to obtain new control outputs. A microgrid control system incorporating SMPC has been presented in [25].

Additional future work includes integration of this formulation with PV, load, and weather forecasts to complete the MPC or SMPC controller as well as integration with the microgrid real-time controller.

Acknowledgment

This work is supported by the Scientific and Technological Research Council of Turkey (TUBITAK) under grant number 119N313.

References

[1] S. Mandelli, J. Barbieri, R. Mereu, and E. Colombo, "Off-grid systems for rural electrification in developing countries: Definitions, classification and a comprehensive literature review," *Renewable and Sustainable Energy Reviews*, vol. 58, pp. 1621–1646, 5 2016.

[2] M. Aliyu, G. Hassan, S. A. Said, M. U. Siddiqui, A. T. Alawami, and I. M. Elamin, "A review of solar-powered water pumping systems," *Renewable and Sustainable Energy Reviews*, vol. 87, pp. 61–76, 5 2018.

[3] D. H. Muhsen, T. Khatib, and F. Nagi, "A review of photovoltaic water pumping system designing methods, control strategies and field performance," *Renewable and Sustainable Energy Reviews*, vol. 68, pp. 70–86, 2 2017.

[4] S. Chandak and P. K. Rout, "The implementation framework of a microgrid: A review," *International Journal of Energy Research*, vol. 45, pp. 3523–3547, 3 2021.

[5] S. Choudhury, "A comprehensive review on issues, investigations, control and protection trends, technical challenges and future directions for microgrid technology," *International Transactions on Electrical Energy Systems*, 2020. [Online]. Available: https://doi.org/10.1002/2050-7038.12446

[6] F. A. Bhuiyan, "Optimal sizing and power management strategies of islanded microgrids for remote electrification systems," *Thesis*, 2014. [Online]. Available: http://ir.lib.uwo.ca/etd

[7] J. Reca-Cardeña and R. López-Luque, *Design Principles of Photovoltaic Irrigation Systems*. Elsevier, 2 2018, vol. 1, pp. 295–333.

[8] S. M. Dawoud, X. Lin, and M. I. Okba, "Hybrid renewable microgrid optimization techniques: A review," *Renewable and Sustainable Energy Reviews*, vol. 82, pp. 2039–2052, 2 2018. [Online]. Available: http://dx.doi.org/10.1016/j.rser.2017.08.007

[9] A. Ghasemi, "Coordination of pumped-storage unit and irrigation system with intermittent wind generation for intelligent energy management of an agricultural microgrid," *Energy*, vol. 142, pp. 1–13, 1 2018.

[10] A. Shoeb and G. M. Shafiullah, "Renewable energy integrated islanded microgrid for sustainable irrigation-a bangladesh perspective," *Energies*, vol. 11, 2018. [Online]. Available: www.mdpi.com/journal/energies

[11] T. Wang, H. Kamath, and S. Willard, "Control and optimization of grid-tied photovoltaic storage systems using model predictive control," *IEEE Transactions on Smart Grid*, vol. 5, pp. 1010–1017, 3 2014.

[12] Güneşköy. [Online]. Available: https://www.guneskoy.org.tr/en/guneskoy/about-guneskoy-2

[13] INVT, *Goodrive100-PV Series Solar Pumping VFD Operation Manual*. [Online]. Available: https://www.invt.com/uploads/file1/20200628/GD100-PV%20Series%20Solar%20Pumping%20VFD%20Manual.pdf

[14] Growatt, *Off Grid Solar Inverter SPF 3500 ES SPF 5000 ES User Manual*. [Online]. Available: https://www.ginverter.com/upload/file/contents/2021/09/61418e6c5e0aa.pdf

[15] U. C. Yilmaz, M. E. Sezgin, and M. Gol, "A model predictive control for microgrids considering battery aging," *Journal of Modern Power Systems and Clean Energy*, vol. 8, pp. 296–304, 2020. [Online]. Available: https://ieeexplore.ieee.org/document/8913672

[16] P. D. Brown and M. Göl. (2022) Software repository for operational optimization of an agricultural microgrid. [Online]. Available: https://github.com/pdb5627/UPEC2022-microgrid-optimization-paper

[17] ——. (2022) Reproducible computing container for operational optimization of an agricultural microgrid. [Online]. Available: https://codeocean.com/capsule/5295207/tree/v1

[18] W. E. Hart, J.-P. Watson, and D. L. Woodruff, "Pyomo: modeling and solving mathematical programs in python," *Mathematical Programming Computation*, vol. 3, pp. 219–260, 2011.

[19] M. L. Bynum *et al.*, *Pyomo–optimization modeling in python*, 3rd ed. Springer Science & Business Media, 2021, vol. 67.

[20] K. Bestuzheva *et al.*, *The SCIP Optimization Suite 8.0*, 12 2021. [Online]. Available: http://www.optimization-online.org/DB_HTML/2021/12/8728.html

[21] Logics and integer-programming representations - yalmip. [Online]. Available: https://yalmip.github.io/tutorial/logicprogramming

[22] B. Chachuat. Mixed-integer linear programming (milp): Model formulation mixed-integer linear programming integer programs (ip). [Online]. Available: http://macc.mcmaster.ca/maccfiles/chachuatnotes/07-MILP-I_handout.pdf

[23] *GNU Linear Programming Kit, Version 5.0*. [Online]. Available: http://www.gnu.org/software/glpk/glpk.html

[24] A. Mesbah, "Stochastic model predictive control: An overview and perspectives for future research," *IEEE Control Systems Magazine*, vol. 36, pp. 30–44, 2016.

[25] S. R. Cominesi, M. Farina, L. Giulioni, B. Picasso, and R. Scattolini, "Two-layer predictive control of a micro-grid including stochastic energy sources," in *2015 American Control Conference (ACC)*, 2015, pp. 918–923.